

REFERENCE STRESS ESTIMATION FOR ANISOTROPIC MATERIALS USING LINEAR ELASITC FINITE ELEMENT RESULTS

Brent M. Scaletta

Solar Turbines Incorporated
 San Diego, California, USA

Dr. Richard Green

Solar Turbines Incorporated
 San Diego, California, USA

ABSTRACT

Components in the hot section of a gas turbine engine experience extended high temperature dwells and cycles composed of multiple starts, changes in load, and variable duration. These loading profiles can lead to damage from cyclic viscoplasticity which is heavily path dependent as dwell stress, yield strength, and stress range change constantly during operation. Since an accurate prediction of accumulated damage is critical to managing an engine, reduced order methods for tracking material behavior over complex operation cycles are necessary tools to help avoid unplanned down time and optimize cost over the operational period.

One method for tracking the material behavior during path dependent cyclic viscoplasticity requires the use of reference stress. Reference stress is a bulk representative stress that can be used in conjunction with various lifing methodologies to determine component durability. Previous papers provided a method for calculating reference stress for isotropic materials using limit load estimation. The goal of this paper is to extend these methodologies to a reference stress estimation method for anisotropic materials to estimate life for single crystal turbine blades. Derived equations will be shown and results from simple Finite Element (FE) test cases will be discussed to demonstrate the accuracy of the anisotropic reference stress estimation.

Once reference stress is obtained, the long term forward creep stress of a component can be estimated for any given initial stress state. This approach can be used to calculate damage during shakedown resulting from redistribution and relaxation due to plasticity and creep, which can be critical for accurately predicting remaining useful life and optimizing engine management.

NOMENCLATURE

σ_{ref}	Reference Stress
σ_{Hill}	Hill Equivalent Stress
P	Applied Load
P_L	Limit Load
σ_e	von Mises Equivalent Stress
ϵ_e	von Mises Equivalent Strain

σ_y	Yield Strength
Y_T	Tensile Yield Strength
Y_S	Shear Yield Strength
m	Exact Limit Load Multiplier
m^0	Upper Bound Limit Load Multiplier
m'	1st Approximation of Limit Load Multiplier
m''	2nd Approximation of Limit Load Multiplier
s_{ij}	Stress Tensor
s_{ij}^0	Stress Tensor at Bulk Plasticity
e_{ij}	Strain Tensor
μ	Plastic Flow Parameter
f	Yield Criteria
f^0	Yield Criteria at Bulk Plasticity
dV	Differential Volume
ΔV	Element Volume
V_T	Total Component Volume
V_s	Redistribution Region Subvolume
C_{ijkl}	Material Constant
G	Approximate Correction Factor
G_μ	Exact Correction Factor
u	Strain Energy Density
ρ	Capacity Parameter
Ω	Critical Strain Energy Density
E	Elastic Modulus
W	Work
ϕ_0	Lagrange Multiplier at Bulk Plasticity
Kt	Stress Concentration
\vec{R}	Applied Load Direction
\vec{r}	Material Orientation of Primary Axis
θ	Load-Material Misalignment
i, j, k, l	Tensor Indices from 1-3
n	Element Number Index
N	Total number of elements

INTRODUCTION

Industrial gas turbine operators are dependent on the availability of their equipment for successful operation of their business. Unplanned down time is costly, disruptive, and represents a significant risk, therefore, equipment reliability is of utmost importance to the operator. From an OEM perspective, reliability represents a critical aspect of meeting a fundamental need and ensuring customer satisfaction. The evolving energy market is demanding more flexibility in operation in order to remain competitive. The industrial gas turbine is therefore required to successfully operate under increasing flexible applications, challenging the initial design assumptions for base load application.

Traditionally, operational risk is addressed in part, through the correct application of conservatism during the initial design phase, followed by scheduled maintenance (based on operation hours), which are typically formulated through a combination of operational experience and engineering assumptions. These assumptions are usually conservative and can be obstructive to operational flexibility. However, as operators expect more capability and value from their industrial units, it has become imperative that OEMs develop technology and analytical modelling capabilities in order to maximize value for customers. Transitioning to condition based maintenance and service models using digital assets to manage equipment health is one such approach. The digital asset is a virtual representation of the physical asset which uses physics based and mathematical models to simulate key functionalities of the physical asset in real time. In the case of industrial gas turbines, this would be key characteristics, such as performance or durability.

Predicting durability in real time is a significant challenge that requires the translation of measured machine operating data, such as gas path temperatures or speed, into relevant engineering parameters. By translating machine data into stress and strain it is possible to predict damage accumulation and therefore remaining useful life, which is key to condition based assessment. Reduced order models are needed to perform these calculations in real time. Traditional approaches such as FEA are computationally inefficient and impractical for this purpose. Surrogate models or representative models which are computationally efficient and fast are central to successfully apply this condition based approach. Reference stress is one such technique which has many uses, including limit load determination, crack initiation, crack propagation, gross deformation, and creep rupture which are all aspects of determining durability. For this reason, the ability to calculate reference stress for anisotropic materials is an important step for applying reduced order methods for predicting the remaining useful life of single crystal turbine blades.

Hari Manoj Simha and Adibi-Asl [1] have organized and concisely laid out the method by which limit load should be estimated for isotropic materials of general form and applied load. This paper expands on their work to extend the methodology to anisotropic limit load prediction which can be used to estimate reference stress for anisotropic materials.

The anisotropic nature of single crystal turbine blades provides many benefits for high temperature applications, such as creep resistance. The Anisotropy also introduces unique challenges to accurately predicting the inelastic stress state due to orientation dependent material properties. The approach presented in the following sections attempts to account for this behavior.

REFERENCE STRESS

Reference stress is a representative bulk stress that can be defined as

$$\sigma_{ref} = \frac{P}{P_L} \sigma_y \quad (1)$$

where P is the applied load, P_L is the limit load, and σ_y is the yield strength. The exact limit load multiplier, m , is defined as

$$m = \frac{P_L}{P} \quad (2)$$

This definition of m is a limit load safety factor based on load rather than stress. Therefore m is the multiplier that will increase the stress state to the point of bulk material failure by means of plastic collapse. Substituting m into (1) gives

$$\sigma_{ref} = \frac{1}{m} \sigma_y \quad (3)$$

Since σ_y is known, solving m is the key to determining reference stress. For that reason, this paper will focus on solving and verifying the value of m .

ANISOTROPIC YIELD CRITERIA

While the method shown in this paper can be used for any yield criteria, the Hill yield criteria was selected because it provided a unified yield condition that could be solved for when applied in the baseline functionals and it could be adapted to single crystal application. The Hill yield criteria is defined as

$$f(s_{ij}) = \frac{1}{2} C_{ijkl} s_{ij} s_{kl} - 1 \quad (4)$$

Using the Hill yield criteria negates the validity of using von Mises equivalent stress which is associated with the von Mises yield criteria. Instead, Hill equivalent stress (σ_{Hill}) will be used where

$$\sigma_{Hill} = \sqrt{\frac{1}{2} [(s_{22} - s_{33})^2 + (s_{33} - s_{11})^2 + (s_{11} - s_{22})^2] + \frac{Y_T^2}{Y_S^2} [s_{23}^2 + s_{31}^2 + s_{12}^2]} \quad (5)$$

LIMIT LOAD ESTIMATION

Mura et al. [5] derived an equation for the exact limit load multiplier, m , using a functional that relates internal and

external energy rate and by solving for the natural conditions. The expression for m was given as

$$m = \int_V s_{ij} \mu \frac{\partial f}{\partial s_{ij}} dV \quad (6)$$

At this point in the limit load analysis, the yield function has been maintained as the generic variable, f . Therefore, any yield condition can be applied at this point. To adapt this methodology to an anisotropic material, the derivative of the general Hill yield criteria would be applied such that

$$\frac{\partial f}{\partial s_{ij}} = C_{ijkl} s_{kl} \quad (7)$$

Remembering that, at yield, $C_{ijkl} s_{ij} s_{kl} = 2$ results in

$$m = 2 \int_{V_T} \mu dV \quad (8)$$

Equation (8) was also obtained by Rimawi et al. [2].

Mura et al. [5] demonstrated that the baseline functional could be distilled down to

$$F = m^0 - \int_{V_T} \mu^0 \{f(s_{ij}^0) + (\phi^0)^2\} dV \quad (9)$$

where m^0 , μ^0 , s_{ij}^0 , and ϕ^0 represent an admissible solution to the functional. Keeping in line with previous notation, the 0-superscript state describes the condition present at bulk plastic collapse, assuming that the entire region has reached the yield strength. The bulk plastic collapse condition can be related to any existing, nonzero stress state (s_{ij}) using

$$s_{ij}^0 = m^0 s_{ij} \quad (10)$$

where m^0 is the upper bound limit load multiplier that causes the entire region to undergo plastic collapse. This term is called the upper bound limit load multiplier because it assumes that load is evenly distributed throughout the whole region at the moment of plastic collapse. Substituting this relationship into the Hill yield criteria gives

$$f(s_{ij}^0) = \frac{1}{2} C_{ijkl} (m^0 s_{ij}) (m^0 s_{kl}) - 1 \quad (11)$$

Finally, equation (11) can be substituted into (9) and the functional can be solved to determine the natural conditions. Combining natural conditions gives

$$m^0 = \frac{1}{\sqrt{\frac{1}{2} C_{ijkl} s_{ij} s_{kl}}} \quad (12)$$

Equation (12) provides an easy convenient way to estimate limit load, but in reality, components do not evenly distribute load in the failure region prior to plastic collapse. For that reason, a more detailed method is needed to better estimate the load carrying capacity of the failure volume at the moment of plastic collapse. By taking two admissible stress states and applying them to the functional (9), Mura et al. [5] were able to relate the upper bound limit load multiplier to the exact multiplier, m , to get the following expression

$$m^0 \leq m \left(1 + \frac{1}{m} \int_{V_T} \mu f^0 dV \right) \quad (13)$$

Equation (13) contains an inequality because an approximation was made by removing a small term containing μ . To replace the inequality with a definitive equation, a new term, m' , is defined where $m' \leq m$. Rearranging equation (13) with m' gives

$$m' = \frac{m^0}{1 + \frac{1}{m} \int_{V_T} \mu f^0 dV} \quad (14)$$

Substituting in the value of m from (8) gives

$$m' = \frac{m^0}{1 + \frac{1}{2} \left[\frac{\int_{V_T} \mu f^0 dV}{\int_{V_T} \mu dV} \right]} \quad (15)$$

Which can be condensed by introducing the term G_μ per Seshadri et al. [3].

$$m' = \frac{m^0}{1 + G_\mu} \quad (16)$$

where

$$G_\mu = \frac{1}{2} \left[\frac{\int_{V_T} \mu f^0 dV}{\int_{V_T} \mu dV} \right] \quad (17)$$

The plastic flow parameter, μ , is a Lagrangian multiplier and its presence produces more unknowns than equations. In order to continue on with the estimation of m' for isotropic materials, Seshadri et al. [3] applied the Schwarz inequality. Repeating that method for the anisotropic G_μ gives

$$G_\mu \leq \frac{1}{2} \sqrt{\frac{\int_{V_T} (f^0)^2 dV}{V_T}} \quad (18)$$

Introducing G such that $G_\mu \leq G$ and applying the Hill yield criteria results in

$$G = \frac{1}{2} \sqrt{\frac{\int_{V_T} \left[\frac{1}{2} (m^0)^2 C_{ijkl} s_{ij} s_{kl} - 1 \right]^2 dV}{V_T}} \quad (19)$$

Applying G to the limit load estimation equation gives the following inequality.

$$m' \geq \frac{m^0}{1 + G} \quad (20)$$

Therefore, another term, m'' , is defined such that $m'' \leq m'$. Substituting m'' into the equation gives

$$m'' = \frac{m^0}{1 + G} \quad (21)$$

Since $m'' \leq m' \leq m$, the estimation of the limit load multiplier is two approximations removed from the exact value. However, the estimation should always be less than the actual limit load value, which produces a known error direction to the limit load prediction method.

BENEFITS OF REDUCED ORDER APPROXIMATIONS

The equations shown in the previous section are approximations for a reduced order model which can be applied to a linear elastic finite element model to get the reference stress for a location of interest. The reference stress can in turn be used in a reduced order lifing methodology to eliminate the need to run finite element models for all possible load conditions.

The ability to run a single load step elastically and apply the limit load calculation to get the reference stress is a significant benefit of this method. In most cases, the time required to solve a nonlinear elastic-plastic finite element model to plastic collapse is an order of magnitude greater than the time required to solve a linear elastic model. In the test cases used for this paper, the nonlinear elastic-plastic solutions time was a factor of fifty greater than the linear elastic models. For a traditional finite element model encompassing multiple components in a gas turbine assembly, solving for nonlinear plastic collapse is impractical, especially when considering multiple load cases. Therefore, joining a reduced order approximation to estimate reference stress with a reduced order lifing method presents a practical solution.

REDISTRIBUTION REGION SELECTION

The subvolume concept was proposed by Seshadri et al. [4] and demonstrated by Hari Manoj Simha and Adibi-Asl [1] who showed that using a subvolume region greatly increased the accuracy of the limit load prediction. When estimating limit load, the selected subvolume region can be referred to as the failure region or the region of plastic collapse, but these terms are not useful when dealing with reference stress which is typically calculated for structures that are far from plastic collapse. Instead, it is helpful to refer to this region as the

redistribution region, because the load will redistribute throughout this region with the accumulation of inelastic strain. Hari Manoj Simha and Adibi-Asl [1] used the relationship

$$\Delta V \in V_s \quad \text{if and only if} \quad \frac{1}{2} \frac{(\sigma_e^2)_n}{E} \frac{1}{\rho} \geq \Omega \quad (22)$$

where n in this case is the index for the n th element and

$$\Omega = \frac{1}{2} \frac{\sigma_y^2}{E} \quad \rho = \frac{W}{\Omega V_T} \quad W = \sum_{n=1}^N \frac{1}{2} (\sigma_e \varepsilon_e) \Delta V_n \quad (23)$$

Using algebraic manipulation simplifies the criteria to

$$\Delta V \in V_s \quad \text{if and only if} \quad \frac{1}{2} \left(\frac{\sigma_e}{E} \right)_n \geq \frac{W}{V_T} \quad (24)$$

This form of the condition shows that an element is considered part of the redistribution volume if its strain energy density is greater than the component's average strain energy density. While the concept is straight forward, the application of the concept using this form of the equation is impractical for two reasons. First, when dealing with either isotropic or anisotropic components in actual applications, material properties tend to vary greatly over the component due to temperature variations. Second, for anisotropic components, the material properties are directionally dependent. A more practical way to apply this technique to general materials for actual applications is to use a form of strain energy density that is independent of material properties. This can be done by keeping the strain energy density calculation in terms of tensorial stress and strain.

$$u = \int s_{ij} de_{ij} = \frac{1}{2} s_{ij} e_{ij} \quad (25)$$

Using this definition of strain energy density, the criteria can be changed to

$$\Delta V \in V_s \quad \text{if and only if} \quad \frac{u_n}{V_T} \geq \frac{W}{V_T} \quad (26)$$

STRESS CONCENTRATION ESTIMATION

The work done by Hari Manoj Simha and Adibi-Asl [1] showed that the limit load methodology for isotropic materials is relatively insensitive to stress concentrations. The demonstration of this effect in anisotropic materials is important since most of the regions of interest are near stress concentration regions. Stress concentrations for anisotropic materials are

more challenging than they are for isotropic materials because the load direction and the material orientation can be offset. In order to estimate stress concentration factors, the following definition was used

$$Kt = \frac{\sigma_{Hill}}{\sigma_{ref}} \quad (27)$$

TEST CASES

Since reference stress is an abstract concept, there is no easy way to verify reference stress predictions. However, the limit load multiplier, m , can easily be verified. By verifying the estimation of m , the reference stress is indirectly verified since m is the only unknown in the reference stress equation. The steps for verifying m are as follows:

1. Create and run a linear elastic FEM with a generic traction load
2. Use the equations in this paper to estimate the redistribution region and the limit load multiplier, m
3. Use the estimated value of m to calculate the load necessary to induce plastic collapse
4. Change the material to elastic perfectly plastic using a Hill yield criteria
5. Solve the nonlinear FEM with incrementally higher loads until the model does not converge
6. Verify that the model has reached plastic collapse by plotting the accumulated equivalent plastic strain. If plastic strains have accumulated to form a failure region, then the part has undergone plastic collapse
7. Note the final load that caused plastic collapse. This is the actual limit load.
8. Compare the predicted limit load to the actual limit load.

For all test cases, quarter plate symmetry was utilized to cut down the model sizes and speed up nonlinear iterations. The material properties of the test cases were those of a single crystal material commonly used for turbine blades. Each case included a feature of some type at the center of the plate in order to introduce a stress concentration and multiaxial stress state to simulate a typical geometric feature found in industrial gas turbine blades. Plane stress elements were used with a standard thickness of 1". A tensile traction load was applied on the top portion of the plate. For each geometry case, the material orientation (\vec{r}) was modified relative to the load direction (\vec{R}) with a clockwise rotation (θ). From here on out, this rotation θ will be referred to as misalignment and will be in units of degrees.

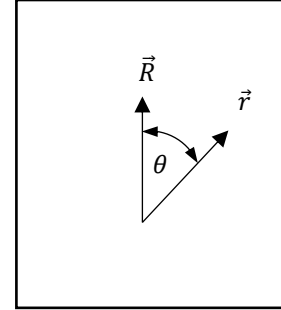


Figure 1: Demonstration of misalignment (θ) between the applied load (\vec{R}) and the material primary axis (\vec{r})

It is worth noting that although single crystal blades are precision cast, some misalignment is expected and therefore the anisotropic model should be capable of managing this type of material misalignment. All of the test cases were analyzed using misalignments of 0° to 45° . While this range is far beyond the expected range of misalignment for single crystal turbine blades, it was important to understand the limitations of the methodology by testing it at extreme bounds.

CASE 1 – STANDARD CENTRAL HOLE

The first test case was the standard central hole model. The hole radius was 0.3" and the width of the quarter plate was 1" from centerline to free edge. The redistribution region was predicted to contain a through section region of the plate, on the side of the hole and a near 45° angle. After solving the nonlinear plastic collapse model, it was seen that the plastic strain accumulation was predominantly within a narrow band on a 45° angle starting at the minimum thickness section near the hole.

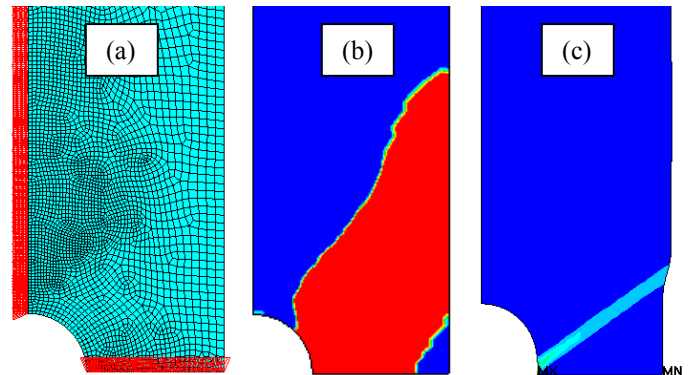


Figure 2: (a) Finite Element Model of the standard central hole case showing symmetry boundary conditions. (b) Linear elastic results showing the predicted redistribution region. (c) Elastic-plastic results showing region of plastic strain accumulation.

Comparisons between the limit load prediction and the nonlinear load at plastic collapse were done at 5° increments until the misalignment reached 45° . The limit load predictions appeared to have a parabolic relationship with misalignment while the nonlinear plastic collapse load had a mild, linear

relationship with misalignment. The calculated error ranged from 4% to 11% with the worst error occurring at a misalignment of 25°. In each case, the predicted limit load was lower than the actual plastic collapse load from the nonlinear model.

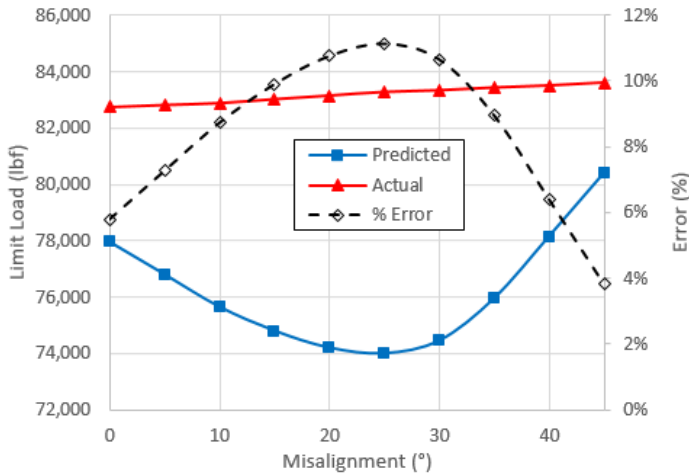


Figure 3: Limit load prediction using derived equations for a standard central hole compared to plastic collapse results from an elastic-plastic analysis with associated error.

The stress concentration for this geometry case range from 1.91 to 2.97 and increase from a misalignment of 0° until 35°. The stress concentration trend appears to be a polynomial with a peak value at a misalignment of 35° and a possible inflection at 0°.

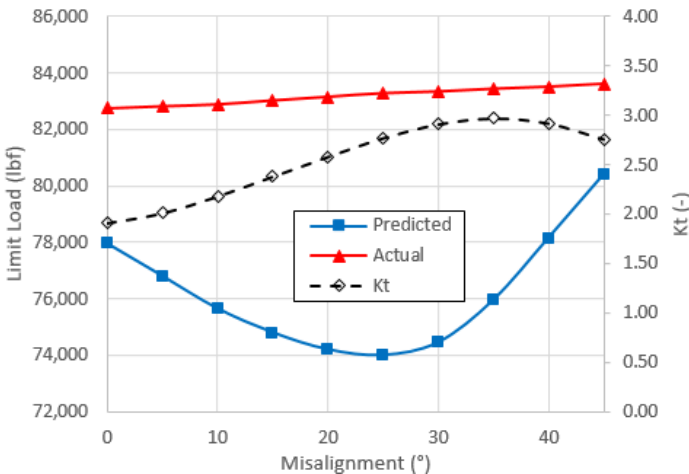


Figure 4: Limit load prediction using derived equations for a standard central hole compared to plastic collapse results from an elastic-plastic analysis with associated stress concentration.

CASE 2 – STANDARD CENTRAL SLOT

The standard central slot case was included to show the effects of having a high stress concentration value. The slot has a radius of 0.1” and extends 0.3” into the 1” wide plate (measured from the centerline to the free edge). The

redistribution region was predicted to contain a through section region of the plate, on the side of the slot and a near 45° angle. After solving the nonlinear plastic collapse model, it was seen that the plastic strain accumulation was predominantly within a narrow band on a 45° angle starting at the minimum thickness section near the hole. The model became unstable before producing a pronounced band as in the case of the standard central hole (case 1).

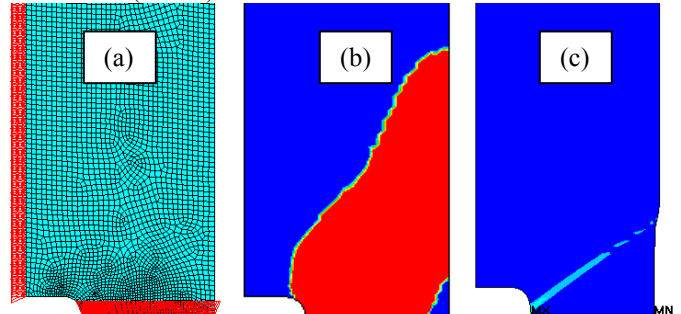


Figure 5: (a) Finite Element Model of the standard central slot case showing symmetry boundary conditions. (b) Linear elastic results showing the predicted redistribution region. (c) Elastic-plastic results showing region of plastic strain accumulation.

Comparisons between the limit load prediction and the nonlinear load at plastic collapse were done at 5° increments until the misalignment reached 45°. The limit load predictions appeared to have an offset parabolic relationship with misalignment and an inflection point at a misalignment of 30°. The nonlinear plastic collapse load also seemed to have an offset parabolic relationship with misalignment, however the inflection point seems to be at a misalignment of 45°. Both curves appear to have similar slopes in the range of 5° to 30°. The calculated error ranged from 2% to 11% with the worst error occurring at 20°. In each case, the predicted limit load was lower than the actual plastic collapse load from the nonlinear model.

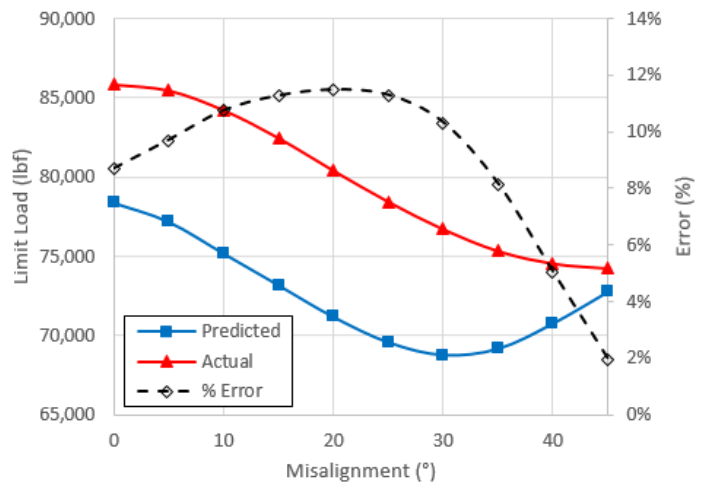


Figure 6: Limit load prediction using derived equations for a standard central slot compared to plastic collapse results from an elastic-plastic analysis with associated error.

The stress concentration factor plotted over misalignment for this case shows a range of 2.97 to 4.48. The trend appears to be a polynomial with inflection points at misalignments of 5° and 35° where the minimum and maximum values occur, respectively.

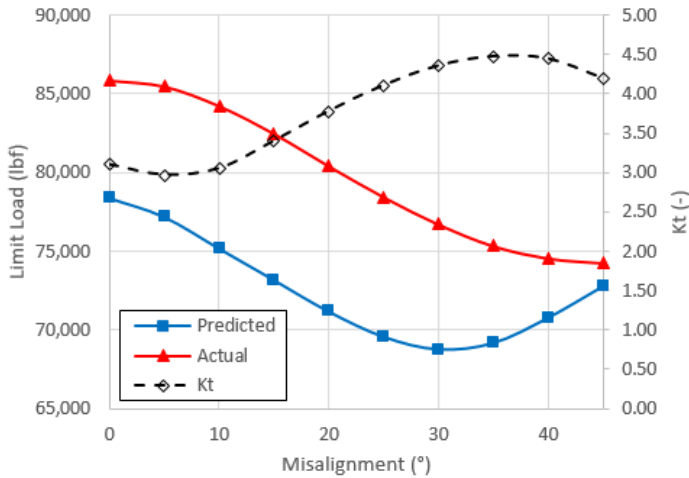


Figure 7: Limit load prediction using derived equations for a standard central slot compared to plastic collapse results from an elastic-plastic analysis with associated stress concentration.

CASE 3 – SHARP CENTRAL SLOT

The central slot case was modified by decreasing the radius to demonstrate higher stress concentration effects. The radius for this case was changed to 0.05” while the depth of the slot remained at 0.3” on a 1” wide plate (measured from centerline to free edge). The redistribution region was predicted to extend from the slot radius to the edge of the plate at a 45° angle. After solving the nonlinear plastic collapse model, it was seen that the plastic strain accumulation was predominantly within a narrow band starting at the slot radius and extending to the plate edge at approximately 45°. The solution became unstable well before the plastic strain band became pronounced as in the standard central hole (case 1). The plastic strain band was even less pronounced (narrower and shorter) than the standard central slot case (case 2).

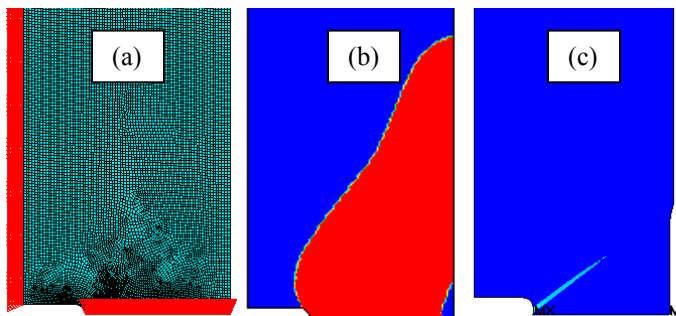


Figure 8: (a) Finite Element Model of the sharp central slot case showing symmetry boundary conditions. (b) Linear elastic results showing the predicted redistribution region. (c) Elastic-plastic results showing region of plastic strain accumulation.

Comparisons between the limit load prediction and the nonlinear load at plastic collapse were done at 5° increments until the misalignment reached 45°. The limit load predictions appeared to have an offset parabolic relationship with misalignment with an inflection point at a misalignment of 30°. The nonlinear plastic collapse load also seemed to have an offset parabolic relationship with misalignment with a possible inflection point near a misalignment of 45°. Both curves appear to have similar slopes in the range of 5° to 30°. The calculated error ranged from 2% to 13% with the worst error occurring at 15°. In each case, the predicted limit load was lower than the actual plastic collapse load from the nonlinear model.

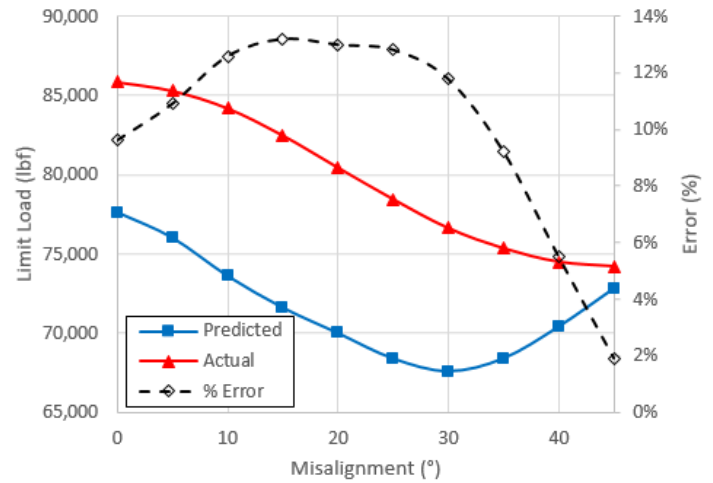


Figure 9: Limit load prediction using derived equations for a sharp central slot compared to plastic collapse results from an elastic-plastic analysis with associated error.

The stress concentration factor plotted over misalignment for this case is within a range of 3.95 to 6.01. The trend appears to be a polynomial with inflection points at 10° and 35° where the minimum and maximum values occur, respectively.

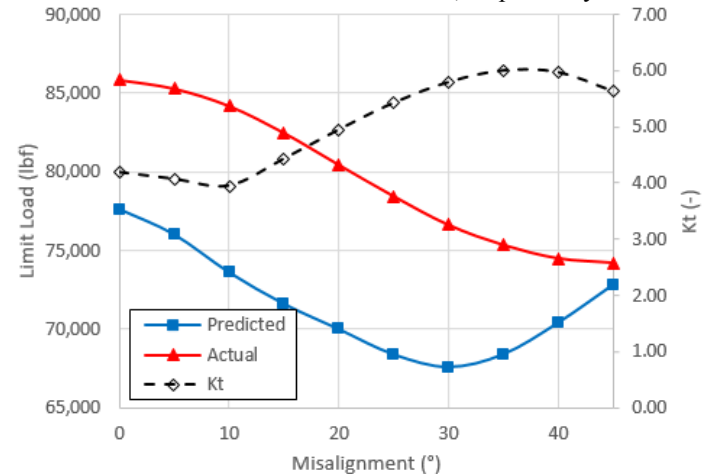


Figure 10: Limit load prediction using derived equations for a sharp central slot compared to plastic collapse results from an elastic-plastic analysis with associated stress concentration.

CASE 4 – SHORT INTERIOR FRACTURE

The short interior fracture was included to demonstrate the limit load predictions for a high stress concentration case. This case was achieved by removing all features and applying boundary conditions all along the edge with the exception of where the fracture occurs. The fracture length used was 0.2” on a 1” wide plate. The redistribution region was predicted to start near the fracture tip and extend across the width of the plate at a 45° angle. After solving the nonlinear plastic collapse model, it was seen that the plastic strain accumulation was predominantly within a narrow band on a 45° angle starting at the tip of the crack and extending across the width of the plate. As in the case of the standard central hole (case 1), a nice even band of plastic strain was formed just prior to plastic collapse.

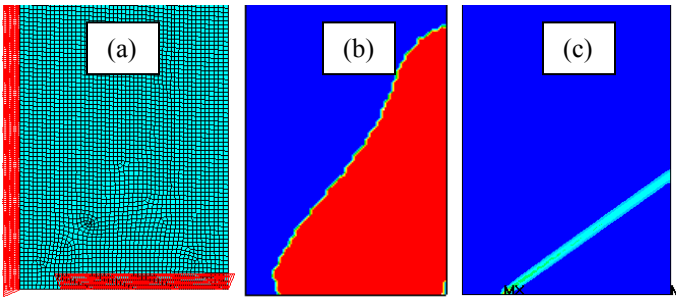


Figure 11: (a) Finite Element Model of the short interior fracture case showing symmetry boundary conditions. (b) Linear elastic results showing the predicted redistribution region. (c) Elastic-plastic results showing region of plastic strain accumulation.

Comparisons between the limit load prediction and the nonlinear load at plastic collapse were done at 5° increments until the misalignment reached 45°. The limit load predictions appeared to have a parabolic relationship with misalignment with an inflection point at a misalignment of 20°. The nonlinear plastic collapse load was relatively unaffected by misalignment having a linear relationship with a slight positive slope. The calculated error ranged from -2% to 18% with the worst error occurring at a misalignment of 20°. In most cases, the predicted limit load was lower than the actual plastic collapse load from the nonlinear model. The limit load prediction was higher than the plastic collapse load at a misalignment of 45°.

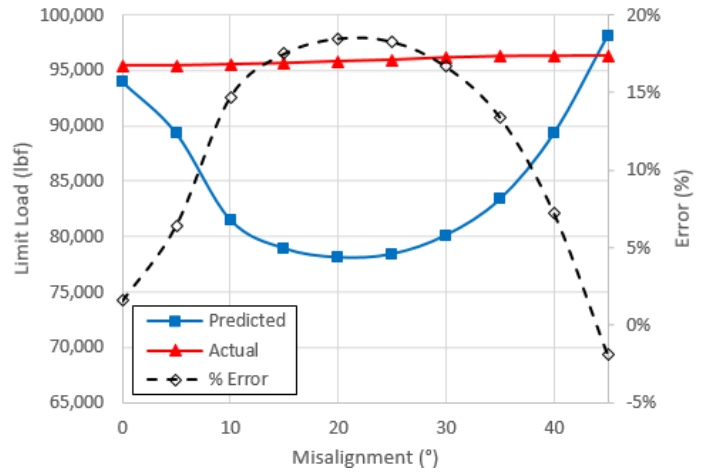


Figure 12: Limit load prediction using derived equations for a short interior fracture compared to plastic collapse results from an elastic-plastic analysis with associated error.

For this test case geometry, the stress concentration value appeared to be relatively constant with a minimum value of 3.73 which occurred at a misalignment of 0° and a maximum value of 3.98 which occurred at a misalignment of 20°.

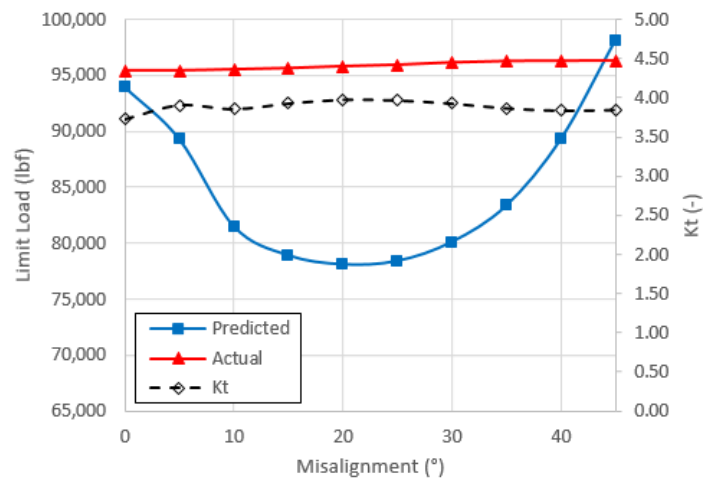


Figure 13: Limit load prediction using derived equations for a short internal fracture compared to plastic collapse results from an elastic-plastic analysis with associated stress concentration.

CASE 5 – LARGE CENTRAL HOLE

The final test case was the large central hole model. The hole radius was 1” and the width of the quarter plate was 2” from the centerline to the free edge. The redistribution region was predicted to contain a through section region of the plate, on the side of the hole and a near 45° angle. After solving the nonlinear plastic collapse model, it was seen that the plastic strain accumulation was predominantly within a narrow band on a 45° angle starting at the minimum thickness section near the hole.

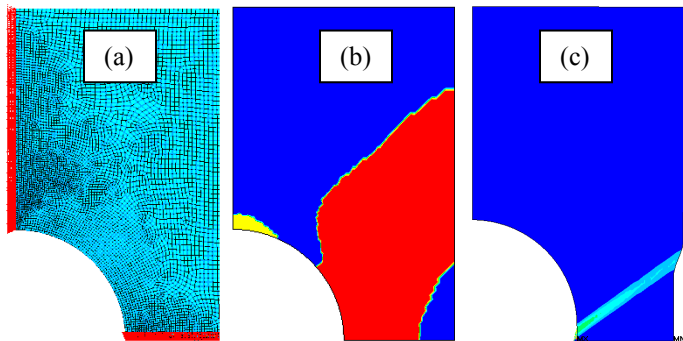


Figure 14: (a) Finite Element Model of the large central hole case showing symmetry boundary conditions. (b) Linear elastic results showing the predicted redistribution region. (c) Elastic-plastic results showing region of plastic strain accumulation.

Comparisons between the limit load prediction and the nonlinear load at plastic collapse were done at 5° increments until the misalignment reached 45°. The limit load predictions appeared to have a parabolic relationship with misalignment while the nonlinear plastic collapse load remained relatively constant with a small increase with misalignment. The calculated error ranged from 13% to 19% with the worst error occurring at 40°. In each case, the predicted limit load was lower than the actual plastic collapse load from the nonlinear model.

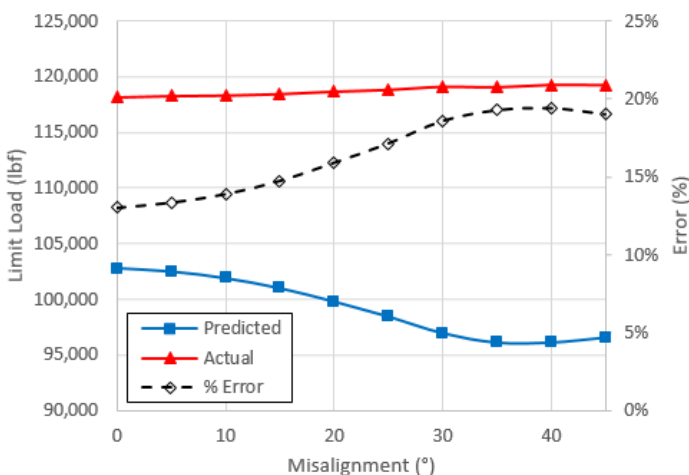


Figure 15: Limit load prediction using derived equations for a large central hole compared to plastic collapse results from an elastic-plastic analysis with associated error.

The stress concentration for this case ranged from 1.72 to 2.52 and increased from a misalignment of 0° until 35°. The stress concentration trend appears to be a polynomial with a peak value at 35°.

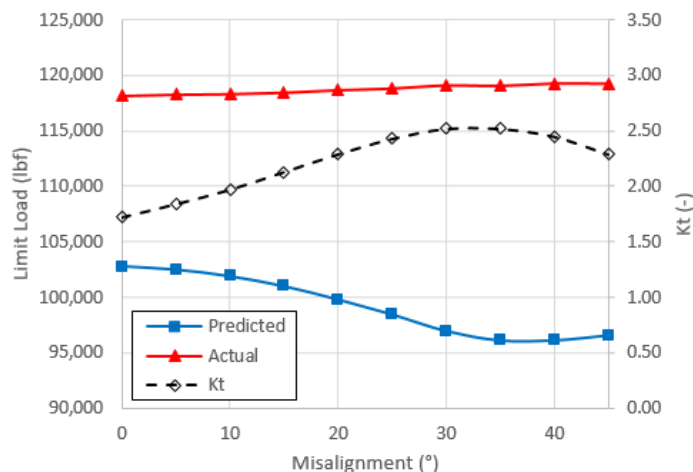


Figure 16: Limit load prediction using derived equations for a large central hole compared to plastic collapse results from an elastic-plastic analysis with associated stress concentration.

DISCUSSION

For most cases, the error associated with a misalignment of 0° was in an acceptable range for predicting limit load. In almost all cases, except for the short crack at a 45° misalignment, the predicted limit load was lower than the actual load at plastic collapse. This is a predictable result as the method calculates m'' and $m'' \leq m' \leq m$, where m is the exact solution. This is also a preferred error if the goal of the analyst is to predict a strength failure. However, if accuracy is more important than conservatism, as in the case of some reference stress based lifing methodologies, there is no preferred direction of error and efforts must be made to understand and minimize the error. In the case of reference stress, the underprediction of limit load results in an over estimation of reference stress.

The largest source of error appears to come from the apparent insensitivity of plastic collapse to misalignment for most components. The components that show this insensitivity are the cases that have well defined bands of plastic strain accumulation on the plane of plastic collapse. Accurate prediction of the plastic collapse trend with misalignment was captured for both slot test cases which both had bands of accumulated plastic strain that were not fully formed on the plane of plastic collapse at the point of instability. This suggests that the method may be more accurate for components that undergo some type of localized plastic collapse than for components that undergo net section plastic collapse with a misalignment greater than 0°.

It is important to note here that the loss of accuracy with misalignment does not necessarily indicate that the methodology cannot handle multiaxial stress conditions. The inclusion of a feature such as a hole, notch, or fracture introduces a multiaxial stress state due to the changing width of the load path. Since all test cases have reasonable accuracy with multiaxial stress states and no misalignment, it is sensible to assume that the error increases with the addition of misalignment for reasons other than multiaxial stress.

The insensitivity to misalignment for components that undergo net section plastic collapse was studied and the observation made was that stress, which is initially influenced by misalignment, becomes realigned with the load direction as plastic strain is accumulated. This phenomenon could be described as a strengthening mechanism for anisotropic materials that exhibit net section plasticity. Since the reference stress method uses the initial elastic stress results, it would not be able to account for this realignment of stress that ultimately influences the limit load capability of anisotropic materials undergoing net section plastic collapse. An explanation for why the limit load prediction for a component with a partially formed band of plastic strain accumulation tracks well with plastic collapse results is that the surrounding elastic material limits the level to which the stress can realign with the load in the region of plastic strain accumulation.

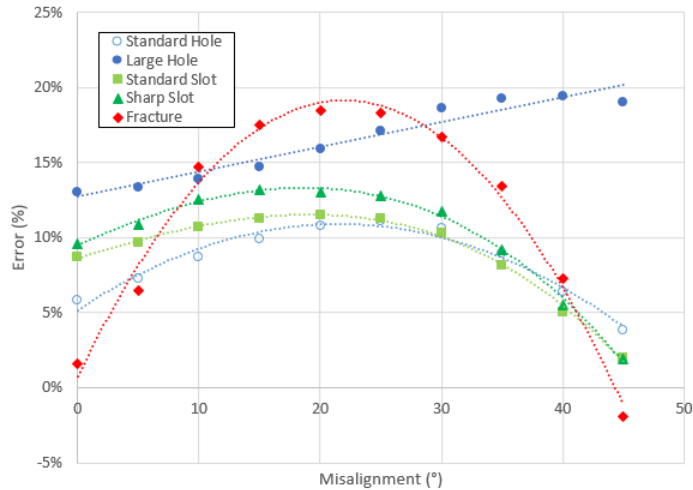


Figure 17: Error in the limit load prediction when comparing nonlinear finite element plastic collapse loads to linear elastic prediction of limit load using the equations shown in this paper. The error results were tracked for each case through various measures of misalignment.

One useful byproduct of the reference stress method is the ability to track stress concentration (Kt) values. Using equation (27) the reference stress was used to estimate Kt for each case at various misalignment conditions. From Figure 18, it can be seen that Kt values for the test cases range from 1.7 to 6 and Kt values vary for the same geometry case as misalignment changes. Comparable geometries had similar trends throughout misalignment, but smaller features had higher Kt values as expected. Surprisingly, the short internal fracture had a lower Kt value than the sharp central slot at all misalignment conditions and a lower Kt value than the standard central slot for misalignment conditions greater than 20°.

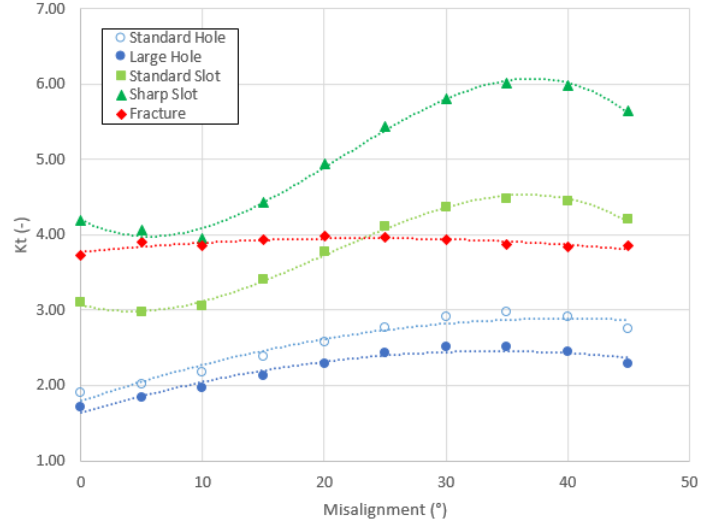


Figure 18: Stress concentration (Kt) estimated using the reference stress method. Estimated Kt values are shown for each case over a range of misalignment conditions.

CONCLUSION

The paper presents a reduced order approach to modeling a complex stress state for anisotropic materials used for single crystal turbine blades in industrial gas turbines engines. This approach is intended to be used in conjunction with other reduced order and surrogate models as part of a digital asset. A digital asset is used to predict remaining useful life in real time, for the purpose of condition based durability assessments. The proposed technique demonstrates significant computational efficiency improvements over traditional full order approaches, which are impractical and computationally inefficient. However, to achieve these computational gains and enable real time calculations, the model fidelity and therefore the accuracy of the solution has been affected.

The consideration then becomes whether the accuracy of the solution is sufficient to achieve the intended purpose. For the proposed solution, the limit load prediction showed a variable loss of accuracy with misalignment, possibly due to strengthening. However, this additional source of error only affects components that are at or near plastic collapse. At intermediate loads, where the plastic strain accumulation has not extended across a net failure section, the stress may not be able to realign with the load, causing the reference stress predictions to be as accurate as the no misalignment case. This trend was seen in both slot test cases where the plastic strain accumulation formed a narrow band that tapered off before reaching the free boundary.

The impact of this observation and loss of fidelity towards the extreme bounds of misalignment is considered to be acceptable for the intended application. The improvements in computational efficiency and calculation speeds are more significant than the loss of fidelity at the bounds of the misalignment for use with turbine blade applications. As the single crystal casting process produces blades with minimal misalignment in the direction of the centrifugal load vector, the

inaccuracies introduced by this approach are tolerable. Furthermore, the inaccuracies can be managed through the effective application of statistical models to provide probabilistic, rather than deterministic results. Where the subsequent stress output is defined with a probability distribution as a function of misalignment. This approach is effective at compensating for inaccuracies in the model.

Given the manageable limitations of the technique it has been shown that the approach can be effectively used for a range of typical features found on industrial gas turbine blades. Test cases 1 through 5 are intended to represent the typical stress state of cast features, such as cooling slots or transition regions around the platforms. Therefore, this technique can be successfully applied to life limiting locations on single crystal turbine blades for the purpose of supporting the remaining useful life calculation.

IMPLICATIONS FOR CONDITION BASED LIFING OF GAS TURBINE COMPONENTS

The reference stress technique is a component of the reduced order modeling approach used to predict the life of industrial gas turbine engine components. Accurate predictions of reference stress are needed to account for damage through creep relaxation/redistribution, cyclic creep perturbation, and forward creep resulting in cyclic viscoplasticity.

These are fundamental aspects of durability and are required to be calculated in order to assess the remaining useful life of key components of an industrial gas turbine. Through the effective application of reduced order models, it is possible to determine the current state of damage, and hence the durability for a specific asset operating in the field. Understanding the condition of the asset relative to how the asset was operated is of significant importance to the owner, operators, and OEM. However, this is only part of the benefit of condition based assessments using digital assets. Adding value to the asset comes in the form of forecasting, or predicting how an asset will respond to intended operation. This allows the operator, in partnership with the OEM, to predict the future state of the asset to assess risk associated with planned operation. This type of capability is extremely valuable when optimizing engine performance, as risk profiles can be created for various scenarios which can be evaluated against the potential value. This type of condition based assessment provided by the digital asset is key to operational flexibility and will become a requirement for future engine management capabilities.

The reference stress technique presented in this paper is one critical element of this overall capability. In order to be confident that our real-time calculations are sufficiently accurate to represent the state of durability within key components, such as single crystal turbine blades, other models and techniques are required to work alongside the reference stress technique. These models and techniques will be discussed in future papers, with the intent to demonstrate how these models can be combined as part of a digital asset, to predict complex material behaviors, such as creep-fatigue interactions, as discussed by Green et al. [12]. Interactions between predominate damage mechanisms can

be significant and must be understood and accounted for in order to achieve sufficiently accurate predictions of durability. Without accuracy and confidence in the capability of the digital asset to represent the physical asset, the resultant predictions may inadvertently introduce risks, which could lead to unintended consequences. Therefore, it is of utmost importance that digital assets are developed and employed by those with the expertise and knowledge of the equipment and intended application which is why the partnership between OEM and Operator is critical.

FURTHER WORK

Upon further review of the results for the test cases, it became apparent that there were some observations that could not be easily explained. More test cases are required to quantify the approach, such as;

- Understand the apparent strengthening mechanism for anisotropic materials that experience net section plastic collapse.
- Test method on components that do not experience net section plastic collapse.
- Include check to verify component experiences subvolume collapse instead of total volume collapse.
- Compare to physical test specimens.

Furthermore, development of an anisotropic rupture reference stress is required in order to effectively predict creep fatigue interactions for single crystal blades using a reduced order approach.

ACKNOWLEDGEMENTS

The authors would like to acknowledge the support of Hari Manoj Simha and Adibi-Asl.

REFERENCES

- [1] Hari Manoj Simha, C., and Adibi-Asl, R., Lower Bound Limit Load Estimation Using a Linear Elastic Analysis, *Journal of Pressure Vessel Technology*, April 2012, Vol. 134
- [2] Rimawi, W.H., Mura, T., and Lee, S.L., Extended Theorems of Limit Analysis of Anisotropic Solids, *Developments in Theoretical and Applied Mechanics*, Proceedings of the Third Southeastern Conference on Theoretical and Applied Mechanics, Vol. 3, 1966, Columbia, SC, USA, pg. 57-71
- [3] Seshadri, R., and Indermohan, H., Lower Bound Limit Load Determination: The m_β -Multiplier Method, *Journal of Pressure Vessel Technology*, Vol. 126, May 2004, pg. 237-240
- [4] Seshadri, R., and Mangalaramanan, S.P., Lower Bound Limit Loads using Variational Concepts: the m_α -method, *Int. J. Pres. Ves. & Piping*, Vol. 71, 1997, pg 93-106
- [5] Mura, T., Rimawi, W.H., and Lee, S.W., Extended Theorems of Limit Analysis, *Q. Appl. Math.*, Vol 23, No. 2, 1965, pg 171-179

- [6] Mura, T., and Lee, S.L., Application of Variational Principles to Limit Analysis, Q. Appl. Math., Vol 21, No. 3, 1963, pg 243-248
- [7] Hill, R., The Mathematical Theory of Plasticity, Oxford University Press, 1950, pg 318-320
- [8] Adibi-Asl, R., Seshadri, R., Elastic Modulus Adjustment Procedures (EMAP) in Metal Forming Analysis, Transactions of the CSME/de la SCGM, Vol. 30, No. 2, 2006
- [9] Fanous, Ihab F.Z., Seshadri, R., Limit Load Analysis Using the Reference Volume Concept, Transactions, SMiRT 19, Toronto, August 2007, Paper #B03/2
- [10] Reinhardt, W.D., Seshadri, R., Limit Load Bounds for the m_α Multiplier, Journal of Pressure Vessel Technology, February 2003, Vol. 125, pg 11-18
- [11] Indermohan, H., Reinhardt, W.D., Seshadri, R., Limit Load of Anisotropic Components Using the M-Beta Multiplier Method, Journal of Pressure Vessel Technology, November 2004, Vol. 126, pg. 455-460
- [12] Green, R.J. and Douglas, J.P., Impact of Engine Operation on Gas Turbine Component Durability using Ductility Exhaustion, The Future of Gas Turbine Technology 8th International Gas Turbine Conference, 12th-13th October 2016, Brussels, Belgium.